

Enhanced adsorptive removal of phosphate on calcined Zr-modified layered double oxide

Yiping Guo^{a,b,c,*}, Weisheng Chen^a, Yong Cao^{a,b}, Guoting Li^{a,b,*}

^aDepartment of Environmental and Municipal Engineering, North China University of Water Resources and Electric Power, Zhengzhou 450011, China, Tel. +86-371-69127538; Fax: +86-371-65790239; emails: guoyiping@ncwu.edu.cn (Y. Guo), lipsonny@163.com (G. Li)

^bHenan Key Laboratory of Water Environment Simulation and Treatment, North China University of Water Resources and Electric Power, Zhengzhou 450011, China

^cDepartment of Molecular Biosciences and Bioengineering, University of Hawaii at Manoa, Honolulu, Hawaii 96822, USA

Received 9 August 2020; Accepted 5 September 2021

ABSTRACT

Layered double hydroxides (LDH) usually performed well for the absorptive removal of phosphate from aqueous solution. In this study, a very limited amount of zirconium (1:100, presumed molar ratio between Zr/LDH) was creatively added into the MgAl-LDH precursor solution before co-precipitation in order to enhance the adsorptive capability of LDH towards phosphate. The uptake of phosphate on the LDH, Zr/LDH, LDO (layered double oxides) LDO and Zr/LDO achieved was 9.19, 10.21, 12.18 and 22.37 mg g⁻¹, respectively. Compared to the raw LDH and the LDO which was the oxidation substrate of layered double hydroxides at 500°C, the adsorption capacity for phosphate by the corresponding LDO and Zr/LDO was improved by 11.1% and 83.7%, respectively. By surface analysis, the synthesized Zr/LDO consists of plate-like particles with sophisticated structures. The introduction of Zr did not change the crystal structures of LDH and LDO by X-ray diffraction analysis. Weakly acidic and neutral solution pH conditions were favorable for phosphate adsorption onto Zr/LDO. By Langmuir model, the calculated maximum adsorption capacity for phosphate at 298 K was 109.4 mg g⁻¹. Thermodynamic analysis indicated that the phosphate adsorption was spontaneous and exothermic, and the coexisting anions and natural organic matter could inhibit the phosphate uptake to some extent.

Keywords: Zirconium; Layered double oxide; Adsorption removal; Phosphate; Characteristic analysis

1. Introduction

Phosphorus is an essential macronutrient that is vital for human beings and animals as well as plants. However, excessive phosphorus has made it one of the main pollutions of wide eutrophication resulted from phosphorus discharge by anthropogenic activities [1]. Eutrophication is one of the phenomena of water pollution that could result in the destruction of the entire aquatic ecosystem, compromise water potability and endanger public health. As such, more

and more stringent effluent standards were established for the allowable phosphate concentration of industrial effluent discharge in China [2]. Hence, the removal and recovery of phosphate are critically necessary for phosphate-bearing wastewater prior to its discharge into the water body. And efficient removal of phosphate from wastewater is of particular significance [3].

Nowadays there are many technologies proposed for efficient phosphate removal, and they can be simply classified as chemical precipitation by using ferric or aluminum salts, biological removal and adsorption according to

* Corresponding authors.

the studies [4–6]. Among these technologies, adsorption is deemed as one appropriate approach due to the convenient, renewable and low-cost properties of adsorbents [7–10]. A large number of adsorbents for phosphate recovery and removals such as iron oxide and hydroxide [11], aluminum hydroxide [12], aluminosilicate [13], calcium silicate [14], sludge waste [15], fly ash [16], metal-loaded orange waste [17] and mango stone biocomposite [18] have been reported. Comparatively speaking, layered double hydroxides (LDH) have attracted intensive attention for phosphate removal as they have exhibited a great potential to remove harmful oxyanions [19]. LDH is composed of stacks of positively-charged, mixed-metal hydroxide layers between which are sandwiched of water molecules and various anionic species that are exchangeable with other aqueous anions in the bulk solution [20]. Based on their unique structures, LDH has the capability for adsorbing a wide range of oxyanions such as phosphate, borate and nitrate from water [19]. Furthermore, calcined LDH and layered double oxides (LDO) usually have a higher adsorption performance as a result of the rehydration and reconstruction processes [21]. Hence, LDH is considered to have the potential application for removing environmental contaminants.

Zirconium and zirconium oxide in different forms had been previously introduced into adsorbents for enhanced removal of arsenic from aqueous solution [22]. In this study, the element zirconium was tentatively incorporated into MgAl-LDH via a facile chemical co-precipitation method to enhance its adsorption capability for oxyanions removal. The introduction of Zr might influence the fundamental structure of MgAl-LDH. In order to maintain the unique structures of MgAl-LDH as much as possible, the presumed molar ratio between Zr and LDH was controlled to be as low as 1:100 during LDH preparation. Both the Zr/LDH and Zr/LDO (calcined at 500°C) were employed for the adsorptive removal of phosphate from water. Scanning electron microscopy, X-ray diffraction patterns and Fourier-transform infrared spectroscopy (FTIR) were conducted to explore the properties of the optimized adsorbent Zr/LDO. A series of batch adsorption experiments were conducted to investigate the effect of solution pH, adsorption kinetics and isotherm to understand the adsorption behavior and mechanism of the Zr/LDO profoundly.

2. Materials and methods

2.1. Materials

Dihydrogen orthophosphate (KH_2PO_4) and other chemicals were purchased from Tianjin Kermel Chemical Reagent Co., Ltd., (Tianjin, China). Other chemicals used including $\text{Mg}(\text{NO}_3)_2$, $\text{Al}(\text{NO}_3)_3$, $\text{ZrOCl}_2 \cdot 8\text{H}_2\text{O}$ were of analytical-reagent grade. Deionized (DI) water was used throughout this study.

2.2. Preparation of adsorbents

Zr-modified layered double hydroxides were prepared via a facile co-precipitation method. Briefly, a 100 mL solution containing $\text{ZrOCl}_2 \cdot 8\text{H}_2\text{O}$ (1:100, presumed molar ratio between Zr and LDH), $\text{Mg}(\text{NO}_3)_2 \cdot 6\text{H}_2\text{O}$, and $\text{Al}(\text{NO}_3)_3 \cdot 9\text{H}_2\text{O}$

($\text{Mg}/\text{Al} = 2.5/1$ (molar ratio)) was added, dropwise and with vigorous stirring, to another 100 mL solution with NaOH and Na_2CO_3 . The pH value of the solution was kept at 8.5–9.5. The slurry was then aged in a water bath at 80°C for 3 h. The precipitate was centrifuged, washed with DI water until the pH of the supernatant was neutral and dried at 80°C overnight. Subsequently, the dry material was ground into fine powder and stored in a desiccator for further use. The Zr/LDH solid was calcined at 500°C for 3 h to obtain the corresponding Zr/LDO500, which was denoted as Zr/LDO in the following tests. Similarly, the Mg/Al LDH and LDO were also prepared as controls [22–24].

2.3. Characterization

The prepared Zr/LDO was characterized with a Philips Quanta-2000 (The Netherlands) scanning electron microscope (SEM) coupled with an energy-dispersive X-ray (EDX) spectrometer. Powder X-ray diffraction (XRD) patterns were recorded on a Rigaku D/MAX-3B X-ray diffractometer (Japan). FTIR spectra (KBr pellets) were recorded on a Nicolet NEXUS 470 FTIR spectrometer (USA) from 400 to 4,000 cm^{-1} . The Zr/LDH500 with a Zr and LDH molar ratio at 1:100 was measured using X-ray photoelectron (PHI 1600 ESCA, Perkin-Elmer Co., USA).

2.4. Batch adsorption experiments

Batch adsorption experiments were conducted in a series of 100 mL conical flasks to investigate the adsorption performance of the Zr/LDO. A stock phosphate solution of 500 mg L^{-1} was prepared by dissolving KH_2PO_4 in DI water. For the test of adsorption isotherm, 10 mg of the Zr/LDO was added into 50 mL of phosphate solution with the concentration range from 2 to 300 mg L^{-1} . And for the test of pH effect, 10 mg of the Zr/LDO was added into 50 mL of phosphate solution with an initial concentration of 5 mg L^{-1} . As preliminary kinetic experiments indicated that 72 h was sufficient to reach the adsorption equilibrium onto Zr/LDO, these flasks were shaken on a horizontal shaker for 72 h at a speed of 140 rpm. In the kinetic study, the beaker containing 1,000 mL of phosphate solution (5 mg L^{-1}) and 200 mg adsorbent were being constantly stirred by a magnetic stirrer. Samples were collected at the desired time interval. The reaction temperature was controlled at a constant temperature of 298 K except for the study on the adsorption isotherm at different temperatures. All the solution pH values were maintained at neutral pH except for the study of the pH effect. The solution pH was adjusted by adding diluted HNO_3 or NaOH solution.

2.5. Analysis methods

The concentration of soluble phosphate of samples, after being filtered through a 0.45 μm syringe filter, was determined photometrically with the molybdenum blue method and then analyzed using an UVmini-1240 spectrophotometer (Shimadzu) by monitoring at the wavelength of maximum absorption (700 nm) [25].

The adsorption capacity (q_e , q_i) was calculated by the following equations:

$$q_e = \frac{(C_0 - C_e)V}{W} \quad (1)$$

$$q_t = \frac{(C_0 - C_t)V}{W} \quad (2)$$

where q_e and q_t (mg g^{-1}) are the adsorption capacity at equilibrium and time t (min), respectively; C_0 , C_e and C_t (mg L^{-1}) are the concentrations of phosphate at the initial stage, equilibrium and t (min), respectively; V (L) is the volume of solution, and W (g) is the mass of the LDH related adsorbents.

3. Results and discussion

3.1. Optimization of the adsorbent

The possible enhancement effect of Zr on the adsorption of phosphate was investigated and compared when the presumed molar ratio between Zr and LDH was only 1:100 for the Zr/LDH and Zr/LDO, as illustrated in Fig. 1. The uptake of phosphate on the LDH, Zr/LDH, LDO and Zr/LDO achieved 9.19, 10.21, 12.18 and 22.37 mg g^{-1} , respectively. Similar to other research on LDH and LDO, calcination at 500°C could increase the specific surface area and the pore volume of LDH [26,27]. Both LDO and Zr/LDO in this research outperformed the corresponding LDH and Zr/LDH for the removal of negatively-charged phosphate. Compared to LDH and LDO, the adsorption capacity for phosphate by the corresponding LDO and Zr/LDO was improved by 11.1% and 83.7%, respectively. The introduction of Zr enhanced the adsorption capability for phosphate removal for both LDH and LDO. As to Zr/LDO, the removal efficiency for phosphate reached as much as 89.5% and the phosphate remaining in the treated solution (5.0 mg L^{-1}) was only 0.525 mg L^{-1} . The reason might be that the introduction of Zr into LDH and LDO could provide more binding sites for phosphate uptake. Totally, the above demonstrates that only a very limited amount of Zr could enhance the adsorption capability

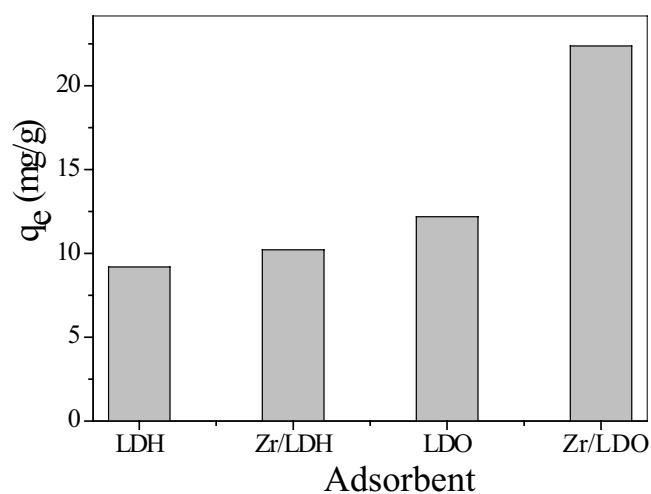


Fig. 1. Effect of Zr content on the adsorption of phosphate.

of LDO significantly, indicating a possible application of Zr/LDO on treating phosphate wastewater. Accordingly, Zr/LDO was selected in the following experiments.

3.2. Adsorbent characterization

The SEM morphologies of Zr/LDO were measured. As presented in Fig. 2, the synthesized Zr/LDO consists of plate-like particles, which is a characteristic morphology of LDO. From Fig. 2b, most of the particles are naturally less than 5 μm , while the thickness of these particles is within 2 μm . From the sophisticated structures of these particles illustrated in Fig. 2c, the fine LDO flakes are few hundred nanometers although they are stacked together compactly. Additionally, from EDS analysis, the average Zr content is up to 0.11% (at%), which is quite close to the Zr content in the precursor solution. The contents of Mg and Al are 16.15% and 7.86% (at%), respectively. The ratio between Mg and Al is 2.05, which is lower than the Mg/Al ratio of 2.5 in the precursor solution.

As shown in Fig. 3, the well-defined powder XRD patterns of Zr/LDH and Zr/LDO show the characteristic reflections of the LDH and LDO phase, indicating that the introduction of Zr did not change the crystal structures of LDH and LDO. The broad diffraction peaks indicate a high degree of crystallinity as well. The diffraction peaks of (110) and (113) at $2\theta = 60^\circ\sim 62^\circ$ is quite clear for Zr/LDH, indicating a high purity of the two adsorbents. Differently, the diffraction peaks at around 29° and 31.5° might contribute to the Zr hydroxides and oxides. Meanwhile, after calcinations treatment, the diffraction peaks of (003), (006) and (009) became not so well-defined as those of the raw Zr/LDH. The diffraction peaks of (110) and (113) on the Zr/LDO almost combined to one peak. These demonstrated that collapses of the layered structures of LDH occurred during calcination treatment, in which the interlayer water and anions were removed and partially mixed metal oxide formed.

The FTIR spectra of Zr/LDH and (b) Zr/LDO were recorded as a comparison, which is presented in Fig. 4. For the two sorbents, there are not typical characteristic absorptions of Zr species. The absorption band at 3,200–3,700 cm^{-1} is attributed to the O–H stretching vibration of the metal hydroxide and interlayer water, while the weak band at 1,626 cm^{-1} corresponds to the bending mode of the absorbed water. The sharp band at 1357 cm^{-1} is typically assigned to the interlayer anions CO_3^{2-} [28,29]. Compared to Zr/LDH, the bands at 554, 636 and 767 cm^{-1} almost disappeared on Zr/LDO due to collapses of layered structures during calcination at 500°C, which indicates the various lattice vibrations associated with metal hydroxide sheets [30].

3.3. Adsorption kinetics under different pH conditions

In order to further understand the adsorption properties, the following kinetic models were utilized to fit the experimental data [31,32]:

Nonlinear pseudo-first-order model

$$q_t = q_e(1 - e^{-k_1 t}) \quad (3)$$

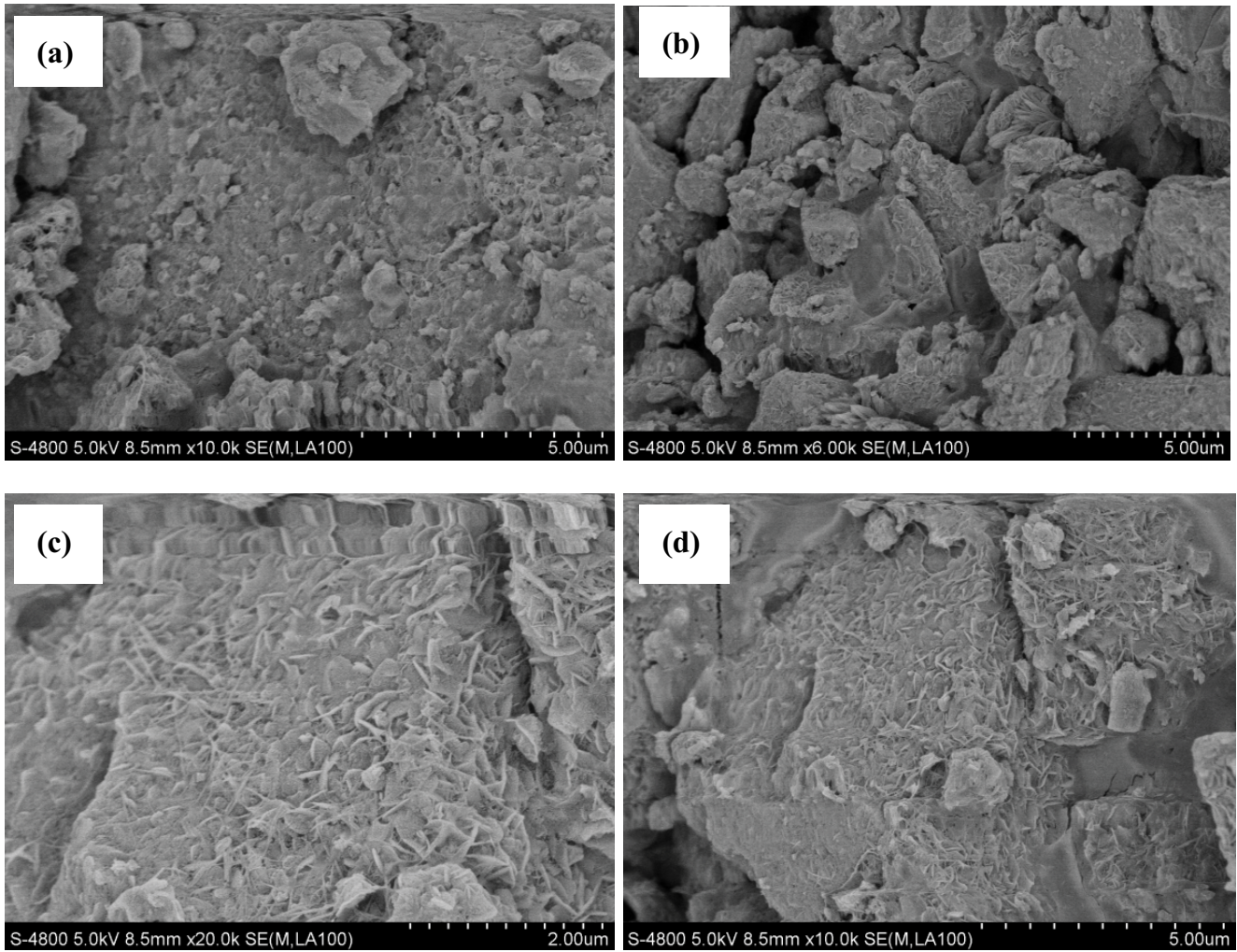


Fig. 2. SEM micrographs of the Zr/LDO under different proportions.

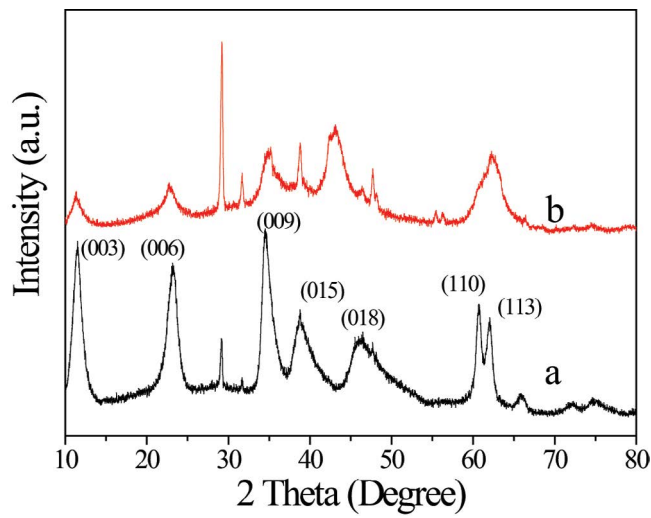


Fig. 3. Powder XRD patterns of (a) Zr/LDH and (b) Zr/LDO.

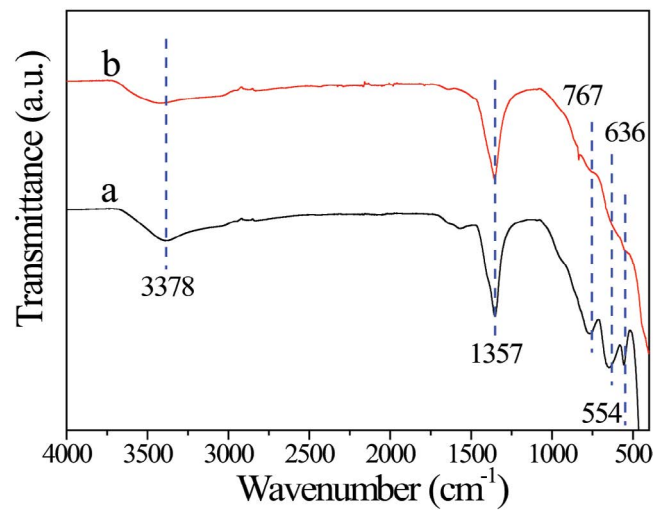


Fig. 4. FTIR spectra of (a) Zr/LDH and (b) Zr/LDO.

Linear pseudo-first-order model

$$\ln(q_e - q_t) = \ln q_e - k_1 t \tag{4}$$

Nonlinear pseudo-second-order model

$$q_t = \frac{k_2 q_e^2 t}{(1 + k_2 q_e t)} \tag{5}$$

Linear pseudo-second-order model

$$\frac{t}{q_t} = \frac{1}{k_2 q_e^2} + \frac{t}{q_e} \tag{6}$$

Elovich model

$$q_t = a + k \ln t \tag{7}$$

where q_e (mg g^{-1}) and q_t (mg g^{-1}) represent the adsorption capacities of the adsorbent at equilibrium and at time t (min), respectively; while k_1 and k_2 mean the related adsorption rate constants for pseudo-first-order and pseudo-second-order

models, respectively; at the same time, a is the constant number and k is adsorption rate constant.

Solution pH usually influences the phosphate uptake on LDH and LDO to a large extent. Herein the effect of solution pH on the adsorption kinetics of phosphate onto Zr/LDO was investigated at pH 5.0, 7.0 and 9.0, respectively. The above kinetic models were used to fit the experimental data.

As demonstrated in Fig. 5a and b, the experimental data was comparatively simulated by linear kinetic models including the pseudo-first-order and pseudo-second-order models. The parameters simulated for the two models are listed in Table 1 as well.

As the pK_1 , pK_2 and pK_3 values of phosphoric acid are 2.15, 7.20 and 12.33, respectively. It can be deduced that, within the pH range of 3.0–10.0, negatively charged H_2PO_4^- and HPO_4^{2-} are the prevailing species of phosphate. As such, below the pH_{pzc} , Zr/LDO is more negatively charged with decreasing solution pH, which facilitates the adsorption of phosphate species evidently. The fitted results are in accordance with the analysis. The correlation coefficients of pseudo-second-order kinetic model were all

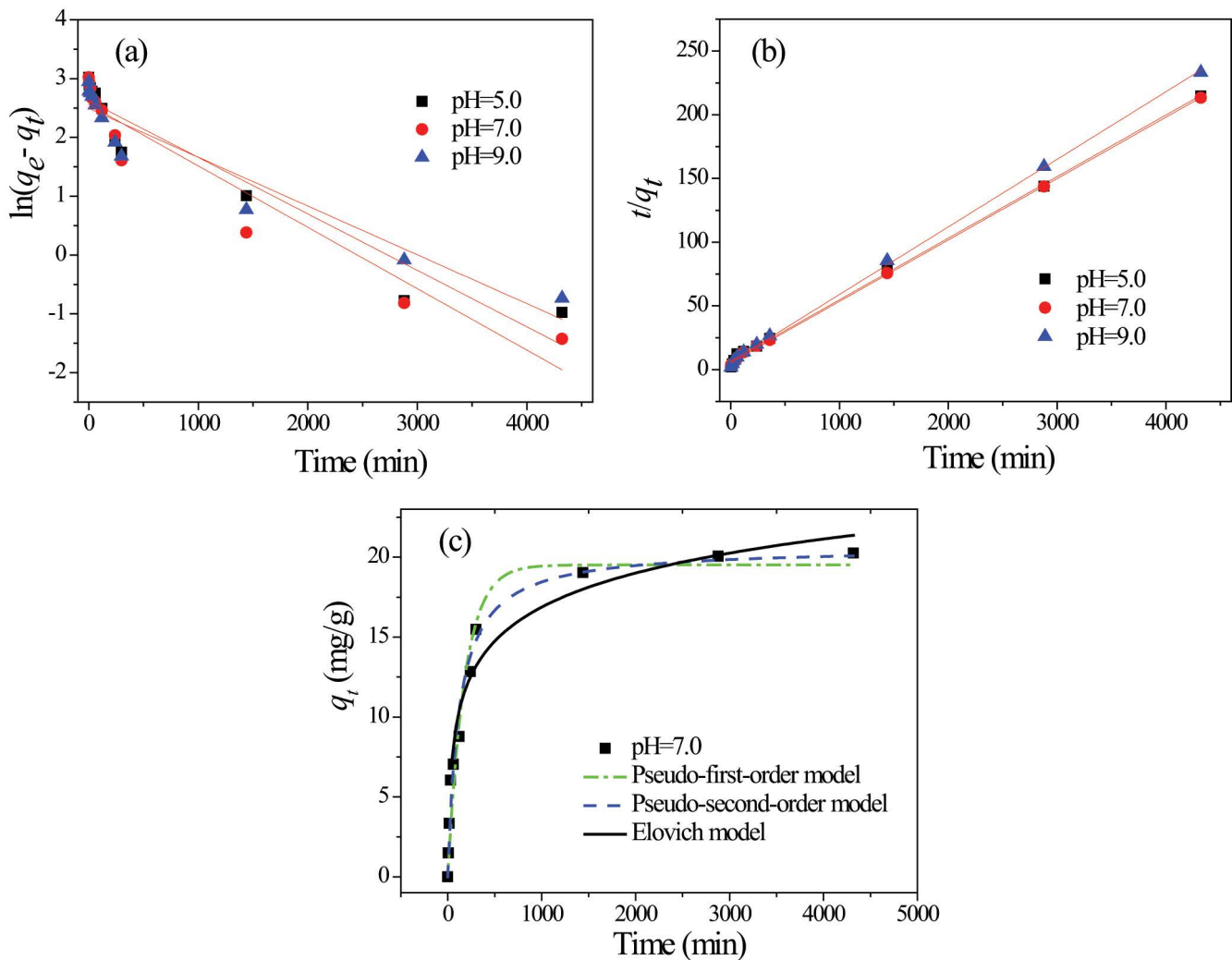


Fig. 7. Linear (a,b) and non-linear (c) adsorption kinetics for pseudo-first-order, pseudo-second-order and Elovich simulation for the adsorption of phosphate onto Zr/LDO.

Table 1
Linear kinetic parameters simulated for the adsorption of phosphate onto Zr/LDO

	Linear pseudo-first-order model			Linear pseudo-second-order model		
	q_e (mg g ⁻¹)	k_1 (min ⁻¹)	R^2	q_e (mg g ⁻¹)	k_2 (mg g ⁻¹ min ⁻¹)	R^2
pH = 5.0	13.75	9.61×10^{-4}	0.915	20.70	3.60×10^{-4}	0.998
pH = 7.0	12.93	1.04×10^{-3}	0.919	20.76	4.37×10^{-4}	0.999
pH = 9.0	12.10	8.30×10^{-4}	0.906	18.86	4.77×10^{-4}	0.999

above 0.998, which was especially higher than those of the pseudo-first-order model. The calculated q_e (mg g⁻¹) values were much close to the experimental values using pseudo-second-order kinetic model. Apparently, pseudo-second-order kinetic model fitted the experimental data better. As pseudo-second-order kinetic model was used to describe chemisorption process, it might be inferred that chemisorption occurred between phosphate molecules and the Zr/LDO surface. In literature, similar kinetic results have been obtained for the adsorption kinetics of various inorganic and organic pollutants on different adsorbent materials [33–35].

Meanwhile, the experimental kinetic data at pH 5.0, 7.0 and 9.0 were fitted by the three non-linear kinetic models, and the simulated curves are also presented in Fig. 5c. At the same time, the calculated kinetic parameters were listed in Table 2. Apparently, it was noted that the pseudo-second-order model fitted the experimental data better than the pseudo-first-order and Elovich kinetic models because the experimental points were much closer to the simulated curves of the pseudo-second-order model. The correlation coefficients (R^2) of the pseudo-second-order model were the highest and most of them were above 0.981, which demonstrated that the overall adsorption process was controlled by a chemisorption process. This conclusion was consistent with the above conclusion derived from the linear pseudo-first-order model and pseudo-second-order model. It should be mentioned that Elovich model suitably described the adsorption kinetics to some extent, in which the rate-determining step might be diffusion in

nature. It could be concluded that chemisorption occurred between phosphate molecules and Zr/LDO adsorbent.

3.4. Adsorption isotherms

As illustrated in Fig. 6, for simplicity, only the adsorption isotherm at 298 K was fitted by the nonlinear Langmuir, Freundlich, Temkin and Redlich–Peterson models. The fitting parameters for the four models were also tabulated in Table 3. The Langmuir adsorption isotherm has been the most widely used adsorption isotherm to express the adsorption of a solute from a liquid solution. The saturated monolayer isotherm can be represented as [36]:

$$q_e = \frac{q_m k_L C_e}{1 + k_L C_e} \quad (8)$$

The Freundlich isotherm, an empirical equation describing the adsorption onto a heterogeneous surface, is commonly presented as [37]:

$$q_e = k_f C_e^{\frac{1}{n}} \quad (9)$$

The Temkin isotherm can be written as [38]:

$$q_e = A + B \ln C_e \quad (10)$$

The three-parameter Redlich–Peterson isotherm equation is proposed to improve the fit by the Langmuir and Freundlich equation and is given by Eq. (11) [39]:

Table 2
Non-linear kinetic parameters simulated for the adsorption of phosphate onto Zr/LDO

Model	pH = 5.0	pH = 7.0	pH = 9.0
Pseudo-first-order model			
k_1 (min ⁻¹)	5.06×10^{-3}	5.6×10^{-3}	5.83×10^{-3}
q_e (mg g ⁻¹)	19.22	19.51	17.55
R^2	0.972; 0.902	0.961; 0.901	0.963
Pseudo-second-order model			
k_2 (g mg ⁻¹ min ⁻¹)	3.36×10^{-4}	4.08×10^{-4}	4.61×10^{-5}
q_e (mg g ⁻¹)	20.59	20.63	18.62
R^2	0.981; 0.971	0.982; 0.967	0.984
Elovich model			
a (g mg ⁻¹ min ⁻¹)	-4.74	-4.36	-3.44
k (mg g ⁻¹)	3.04	3.07	2.70
R^2	0.953; 0.984	0.975; 0.982	0.967

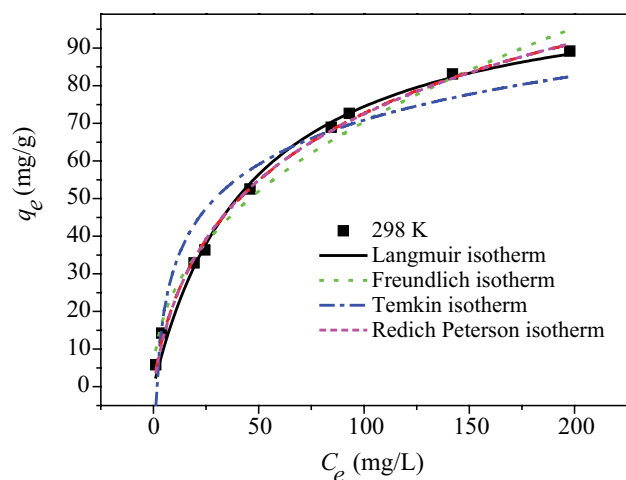


Fig. 6. Simulated Langmuir, Freundlich, Temkin and Redlich–Peterson isotherm curves for the adsorption of phosphate onto Zr/LDO.

$$q_e = \frac{AC_e^n}{1 + BC_e^n} \quad (11)$$

where q_e is the amount of the adsorbed adsorbate (mg g^{-1}) at equilibrium, q_m is the monolayer adsorption capacity of the adsorbent (mg g^{-1}), C_e is the concentration of adsorbate in the solution at equilibrium (mg L^{-1}), k_L is the Langmuir isotherm constant (L mg^{-1}) that is related to the adsorption energy, k_F is the Freundlich constant, $1/n$ is the adsorption intensity, A and B are isotherm constants.

From Fig. 6, generally speaking, Langmuir, Freundlich and Redlich–Peterson models could better fit the experimental data as the experimental points are quite close to the simulated curves. Based on the correlation coefficients (R^2) listed in Table 3, at the three temperatures, the R^2 values from Redlich–Peterson model are the highest among the four isotherm models and this demonstrates that Redlich–Peterson model is the best to fit the experimental data, which is consistent with other study [40]. The R^2 values from Langmuir model are slightly higher than those from Freundlich model, indicating that the phosphate adsorption process on Zr/LDHO was saturated monolayer adsorption to a large extent. From Langmuir model, the calculated maximal adsorption capacities for phosphate at 288, 298 and 308 K were 148.1, 109.4 and 95.5 mg g^{-1} , respectively. It is obvious that the adsorption capacity decreased with increasing temperature, indicating that the adsorption process is exothermic in nature. Similar endothermic adsorption behavior was reported for many adsorbent-pollutant systems in literature [41,42]. Nevertheless, from a practical point of view, Zr/LDO with such a high adsorption capability is expected to be used as an alternative to commercial adsorbents for phosphate recovery and removal from aqueous solutions.

3.5. Effect of natural organic matter and coexisting anions

Natural organic matter and coexisting anions are usually capable of influencing the uptake of phosphate.

Table 3
Simulated isotherm parameters for phosphate adsorption at different temperatures

	288 K	298 K	308 K
Langmuir			
q_{\max} (mg g^{-1})	148.1	109.4	94.5
k_L (L mg^{-1})	0.021	0.021	0.019
R^2	0.997	0.992	0.998
Freundlich			
k_F	11.32	9.35; 9,947	6.87
n	2.17	2.28	2.16
R^2	0.953	0.984	0.975
Temkin			
A	−20.53	−7.03	−11.93
B	25.35	16.91	15.59
R^2	0.937	0.927	0.940
Redlich–Peterson			
A	2.61	3.92	1.97
B	0.00820	0.121	0.0295
g	1.14	0.78	0.94
R^2	0.998	0.994	0.998

The effect of natural organic matter and coexisting anions on phosphate uptake on Zr/LDO was investigated and the results are presented in Fig. 7. Humic acid (HA), as a typical natural organic matter, is a kind of macromolecule organic compound widely existing in natural water body. As illustrated in Fig. 7a, the uptake of phosphate reduced from 20.7 mg g^{-1} in the absence of HA to 17.3 mg g^{-1} in the presence of 5 mg L^{-1} of HA. A slight decrease of 16.4% indicates a weak influence of HA on the phosphate uptake. On the other hand, the ubiquitous coexisting anions such as Cl^- , SO_4^{2-} and HCO_3^- are commonly occurring anions in natural environment, which are supposed to compete with phosphate for active sites of a given adsorbent to some extent. Fig. 7b demonstrates that the total adsorption of phosphate decreased with an increasing concentration of these competing anions. The uptake of phosphate decreased from 20.7 mg g^{-1} in the absence of anions to 17.4, 16.1 and 10.6 mg g^{-1} in the presence of 0.1 M of Cl^- , SO_4^{2-} and HCO_3^- , respectively. The competitive effect of these anions can be ranked in the order $\text{HCO}_3^- > \text{SO}_4^{2-} > \text{Cl}^-$, which agrees with the ionic potential z/r , where z is charge of the anion and r is size of the anion. Nevertheless, due to a higher ionic potential z/r of bi- and tri-valent anions, bi- and tri-valent anions are more competitive than monovalent anions with the exception of HCO_3^- . The reason of HCO_3^- showing a higher influence on phosphate adsorption was probably attributed to the fact that the hydrolysis of CO_3^{2-} increased the competing OH^- concentration and consequently reduced phosphate uptake. Furthermore, in most cases, the presence of the three inorganic anions decreased the adsorption capacity far less than 50%, suggesting that H_2PO_4^- has a high affinity to Zr/LDO and that anion-exchange might not be the predominant mechanism for phosphate adsorption on Zr/LDO.

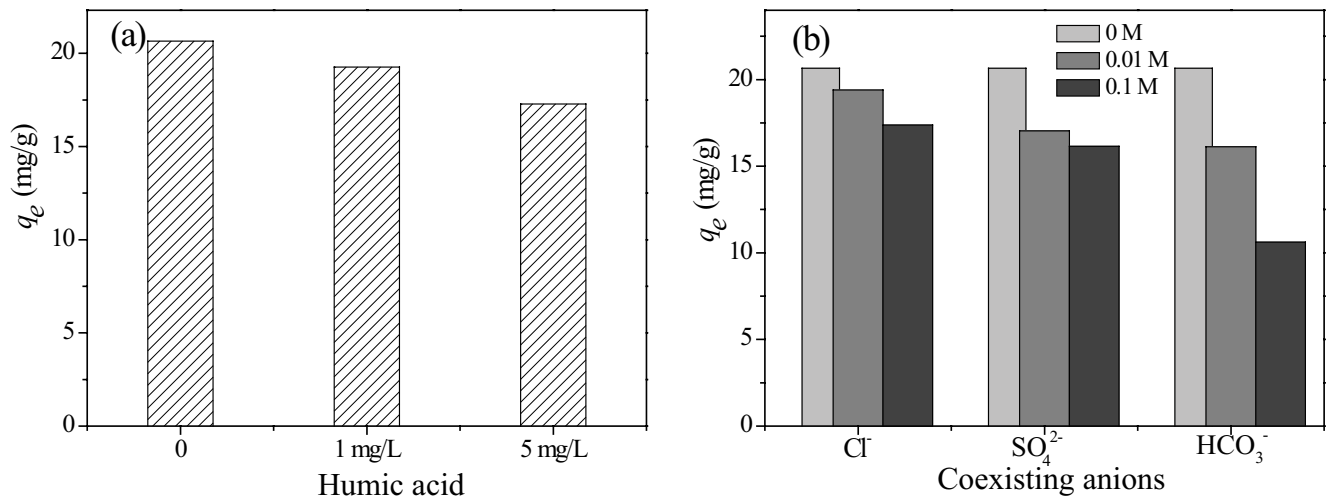


Fig. 7. Effect of natural organic matter (a) and coexisting anions (b) on phosphate adsorption.

4. Conclusion

A very limited amount of zirconium (1:100, presumed molar ratio between Zr/LDH) was creatively introduced into the Mg/Al LDH substrate via a facile co-precipitation method to enhance its adsorption capability towards phosphate. By comparing the adsorption capability of LDH, Zr/LDH, LDO and Zr/LDO, it was found that Zr/LDO, which was subjected to calcination at 500°C, outperformed other adsorbents. By surface analysis, the synthesized Zr/LDO consists of plate-like particles with sophisticated structures. The high adsorption performance was observed at weakly acidic and neutral solution pH. Kinetic analysis indicated that phosphate adsorption on Zr/LDO well fitted by the pseudo-second-order model. The Redlich–Peterson model did the best job to fit the adsorption isotherm data. By Langmuir model, the calculated maximal adsorption capacity for phosphate at 298 K was 109.4 mg g⁻¹. Thermodynamic and kinetic experiments demonstrated that the phosphate adsorption was a spontaneous, exothermic and chemically adsorptive process. The coexisting anions and natural organic matter could inhibit the phosphate uptake to some extent.

Acknowledgement

This research was supported by the National Science Foundation of China (Grant No. 51378205), the foundation from Henan Province Science and Technology Major Project (Grant No. 161100310700), the State Scholarship Fund of China Scholarship Council (Grant No. 201708410476), Introduction plan of high-end foreign experts in Henan Province (Grant No. HNGD2020047), and Open fund of Key Laboratory of water environment simulation and treatment in Henan Province (Grant No. KFJJ201902).

References

- [1] J.-Q. Jiang, N.J.D. Graham, Pre-polymerised inorganic coagulants and phosphorus removal by coagulation – a review, *Water SA*, 24 (1998) 237–244.
- [2] SEPA, The State Standards of Integrated Wastewater Discharge, GB 8978–1996, 1996.
- [3] G.L. Li, S. Gao, G.S. Zhang, X.W. Zhang, Enhanced adsorption of phosphate from aqueous solution by nanostructured iron(III)–copper(II) binary oxides, *Chem. Eng. J.*, 235 (2014) 124–131.
- [4] L.J. Sherwood, R.G. Qualls, Stability of phosphorus within a wetland soil following ferric chloride treatment to control eutrophication, *Environ. Sci. Technol.*, 35 (2001) 4126–4131.
- [5] T. Clark, T. Stephenson, P.A. Pearce, Phosphorus removal by chemical precipitation in a biological aerated filter, *Water Res.*, 31 (1997) 2557–2563.
- [6] A. Oehmen, P.C. Lemos, G. Carvalho, Z.G. Yuan, J. Keller, L.L. Blackall, M.A.M. Reis, Advances in enhanced biological phosphorus removal: From micro to macro scale, *Water Res.*, 41 (2007) 2271–2300.
- [7] H.N. Bhatti, Y. Safa, S.M. Yakout, O.H. Shair, M. Iqbal, A. Nazir, Efficient removal of dyes using carboxymethyl cellulose/alginate/polyvinyl alcohol/rice husk composite: adsorption/desorption, kinetics and recycling studies, *Int. J. Biol. Macromol.*, 150 (2020) 861–870.
- [8] S. Noreen, H.N. Bhatti, M. Iqbal, F. Hussain, F.M. Sarim, Chitosan, starch, polyaniline and polypyrrole biocomposite with sugarcane bagasse for the efficient removal of Acid Black dye, *Int. J. Biol. Macromol.*, 147 (2020) 439–452.
- [9] M.A. Tahir, H.N. Bhatti, I. Hussain, I.A. Bhatt, M. Asghar, Sol-gel synthesis of mesoporous silica-iron composite: kinetics, equilibrium and thermodynamics studies for the adsorption of turquoise-blue X-GB dye, *Z. Phys. Chem.*, 234 (2020) 233–253.
- [10] U. Kamran, H.N. Bhatti, M. Iqbal, S. Jamil, M. Zahid, Biogenic synthesis, characterization and investigation of photocatalytic and antimicrobial activity of manganese nanoparticles synthesized from *Cinnamomum verum* bark extract, *J. Mol. Struct.*, 1179 (2019) 532–539.
- [11] Z.H. Shao, R. Stanforth, Competitive adsorption of phosphate and arsenate on goethite, *Environ. Sci. Technol.*, 35 (2001) 4753–4757.
- [12] S. Tanada, M. Kabayama, N. Kawasaki, T. Sakiyama, T. Nakamura, M. Araki, T. Tamura, Removal of phosphate by aluminum oxide hydroxide, *J. Colloid Interface Sci.*, 257 (2003) 135–140.
- [13] K. Okada, Y. Ono, Y. Kameshima, A. Nakajima, K.J.D. Mackenzie, Simultaneous uptake of ammonium and phosphate ions by composites of γ -alumina/potassium aluminosilicate gel, *Mater. Res. Bull.*, 38 (2003) 749–756.
- [14] D.C. Southam, T.W. Lewis, A.J. Macfaelane, J.H. Johnston, Amorphous calcium silicate as a chemisorbent for phosphate, *Curr. Appl. Phys.*, 4 (2004) 355–358.

- [15] A.K. Golder, A.N. Samanta, S. Ray, Removal of phosphate from aqueous solutions using calcined metal hydroxides sludge waste generated from electrocoagulation, *Sep. Purif. Technol.*, 52 (2006) 102–109.
- [16] J. Chen, H.N. Kong, D.Y. Wu, Z.B. Hu, Z.S. Wang, Y.H. Wang, Removal of phosphate from aqueous solution by zeolite synthesized from fly ash, *J. Colloid Interface Sci.*, 300 (2006) 491–497.
- [17] B.K. Biswas, K. Inoue, K.N. Ghimire, S. Ohta, H. Harada, K. Ohto, H. Kawakita, The adsorption of phosphate from an aquatic environment using metal-loaded orange waste, *J. Colloid Interface Sci.*, 312 (2007) 214–223.
- [18] H.N. Bhatti, J. Hayat, M. Iqbal, S. Noreena, S. Nawaz, Biocomposite application for the phosphate ions removal in aqueous medium, *J. Mater. Res. Technol.*, 7 (2018) 300–307.
- [19] K.H. Goh, T.T. Lim, Z.L. Dong, Application of layered double hydroxides for removal of oxyanions: a review, *Water Res.*, 42 (2008) 1343–1368.
- [20] D.G. Evans, R.C.T. Slade, Structural Aspects of Layered Double Hydroxides, X. Duan, D.G. Evans, Eds., *Layered Double Hydroxides*, Springer Berlin Heidelberg, Berlin, Heidelberg, 2006, pp. 1–87.
- [21] K. Abdellaoui, I. Pavlovic, M. Bouhent, A. Benhamou, C. Barriga, A comparative study of the amaranth azo dye adsorption/desorption from aqueous solutions by layered double hydroxides, *Appl. Clay Sci.*, 143 (2017) 142–150.
- [22] T.A. Khan, S.A. Chaudhry, I. Ali, Thermodynamic and kinetic studies of As(V) removal from water by zirconium oxide-coated marine sand, *Environ. Sci. Pollut. Res.*, 20 (2013) 5425–5440.
- [23] F.R. Costa, A. Leuteritz, U. Wagenknecht, D. Jehnichen, L. Häußler, G. Heinrich, Intercalation of Mg-Al layered double hydroxide by anionic surfactants: preparation and characterization, *Appl. Clay Sci.*, 38 (2008) 153–164.
- [24] R.M.M. dos Santos, R.G.L. Gonçalves, V.R.L. Constantino, C.V. Santilli, P.D. Borges, J. Tronto, F.G. Pinto, Adsorption of Acid Yellow 42 dye on calcined layered double hydroxide: effect of time, concentration, pH and temperature, *Appl. Clay Sci.*, 140 (2017) 132–139.
- [25] State Environmental Protection Administration of China, *Monitoring and Analysis Methods of Water and Wastewater*, 4th ed., China Environmental Science Press, Beijing, 2002, p. 246.
- [26] T. Bujdosó, Á. Patzkó, Z. Galbács, I. Dékány, Structural characterization of arsenate ion exchanged MgAl-layered double hydroxide, *Appl. Clay Sci.*, 44 (2009) 75–82.
- [27] F.R. Costa, A. Leuteritz, U. Wagenknecht, D. Jehnichen, L. Häußler, G. Heinrich, Intercalation of Mg-Al layered double hydroxide by anionic surfactants: preparation and characterization, *Appl. Clay Sci.*, 38 (2008) 153–164.
- [28] Z.M. Bai, Z.Y. Wang, T.G. Zhang, F. Fu, N. Yang, Synthesis and characterization of Co-Al-CO₃ layered double-metal hydroxides and assessment of their friction performances, *Appl. Clay Sci.*, 59–60 (2012) 36–41.
- [29] C. Zhang, S.G. Yang, H.Z. Chen, H. He, C. Sun, Adsorption behavior and mechanism of reactive brilliant red X-3B in aqueous solution over three kinds of hydrotalcite-like LDHs, *Appl. Surf. Sci.*, 301 (2014) 329–337.
- [30] F.R. Costa, A. Leuteritz, U. Wagenknecht, D. Jehnichen, L. Häußler, G. Heinrich, Intercalation of Mg-Al layered double hydroxide by anionic surfactants: preparation and characterization, *Appl. Clay Sci.*, 38 (2008) 153–164.
- [31] Y.S. Ho, G. McKay, Pseudo-second-order model for sorption process, *Process Biochem.*, 34 (1999) 51–65.
- [32] M. Kithome, J.W. Paul, L.M. Lavkulich, A.A. Bomke, Kinetics of ammonium adsorption and desorption by the natural zeolite clinoptilolite, *Soil Sci. Soc. Am. J.*, 62 (1988) 622–629.
- [33] O. Duman, S. Tunc, B.K. Bozoglan, T.G. Polat, Removal of triphenylmethane and reactive azo dyes from aqueous solution by magnetic carbon nanotube-k-carrageenan-Fe₃O₄ nanocomposite, *J. Alloys Compd.*, 687 (2016) 370–383.
- [34] O. Duman, T.G. Polat, C.O. Diker, S. Tunc, Agar/kappa-carrageenan composite hydrogel adsorbent for the removal of Methylene Blue from water, *Int. J. Biol. Macromol.*, 160 (2020) 823–835.
- [35] E. Ayranci, O. Duman, Removal of anionic surfactants from aqueous solutions by adsorption onto high area activated carbon cloth studied by in situ UV spectroscopy, *J. Hazard. Mater.*, 148 (2007) 75–82.
- [36] S. Lagergren, Zur theorie der sogenannten adsorption gelöster stoffe, *Kungliga Svenska Vetenskapsakademiens Handlingar*, 24 (1898) 1–39.
- [37] H.M.F. Freundlich, Über die adsorption in lasungen, *J. Phys. Chem.*, 57 (1906) 385–470.
- [38] X.C. Fu, W.X. Shen, T.Y. Yao, *Physical Chemistry*, 4th ed., Higher Education Press, Beijing, China, 1994, pp. 303–321.
- [39] O. Redlich, D.L. Peterson, A useful adsorption isotherm, *J. Phys. Chem.*, 63 (1959) 1024–1026.
- [40] R.P. Han, J.J. Zhang, P. Han, Y.F. Wang, Z.H. Zhao, M.S. Tang, Study of equilibrium, kinetic and thermodynamic parameters about methylene blue adsorption onto natural zeolite, *Chem. Eng. J.*, 145 (2009) 496–504.
- [41] O. Duman, S. Tunc, T.G. Polat, Adsorptive removal of triarylmethane dye (Basic Red 9) from aqueous solution by sepiolite as effective and low-cost adsorbent, *Microporous Mesoporous Mater.*, 210 (2015) 176–184.
- [42] O. Duman, S. Tunc, T.G. Polat, Determination of adsorptive properties of expanded vermiculite for the removal of C.I. Basic Red 9 from aqueous solution: kinetic, isotherm and thermodynamic studies, *Appl. Clay Sci.*, 109–110 (2015) 22–32.